AIAA 2000-4142

Calculation of Weak Stability Boundary Ballistic Lunar Transfer Trajectories

Edward A. Belbruno,
Princeton University and Innovative Orbital Design, Inc.
Princeton, New Jersey
John P. Carrico,
Analytical Graphics, Inc.
Malvern, Pennsylvania

AIAA/AAS Astrodynamics Specialist Conference
14–17 August, 2000
Denver, Colorado

CALCULATION OF WEAK STABILITY BOUNDARY BALLISTIC LUNAR TRANSFER TRAJECTORIES

Edward A. Belbruno*, John P. Carrico†,

ABSTRACT

Ballistic lunar capture transfers from the Earth were first developed in 1987[1], using the weak stability boundary (WSB) theory. This type of lunar transfer is known commonly as the WSB transfer. In 1991 a WSB transfer was used by the Japanese spacecraft Hiten which successfully reached the Moon in October of that year[2,5,16]. Since that time WSB transfers have been extensively studied, and several missions are planning to utilize its fuel saving properties[5,10]. This recent interest in WSB transfers has motivated finding a more accessible way to generate them. This paper demonstrates the algorithms and methodologies to design WSB transfers and analyze launch windows. This work is being done with the software package STK/*Astrogator*. *Astrogator* is the successor to the well known software package *Swingby,* which was developed at the NASA/Goddard Space Flight Center and has been the subject of several previous papers[7,8,17].

1. INTRODUCTION

Ballistic lunar capture transfers from the earth to the moon have the unique property that upon arrival at the moon, a spacecraft is automatically captured in an elliptical orbit without the use of rockets. Transfers using this process were first precisely numerically demonstrated in 1987[1]. These were initially designed for spacecraft requiring electric propulsion. A more useful transfer of this type for rockets using chemical propulsion was designed in 1990, and used by the Japanese spacecraft Hiten in 1991 which arrived at the Moon in October of that year[2,5,16]. The efficient calculation of this transfer is the subject of this paper. These transfers are of interest for applications because of their fuel saving property.

The transfer used in 1991 has evolved considerably since that time, and is commonly referred to as the WSB lunar transfer. This boundary is a region about the Moon where sensitive chaotic dynamics can occur, and was first numerically discovered and mapped out in 1987[1]. A new analytic approximation has recently been developed and is described in Section 2.2. The WSB can be viewed as a generalization of the Lagrange points and is a complicated region surrounding the Moon. The WSB has been described in more detail[5,6], and a plot of one is shown in Figure 1 represented in an Earth-Centered Inertial (ECI) coordinate system. An object can be ballistically captured at the Moon if it arrives at the WSB.

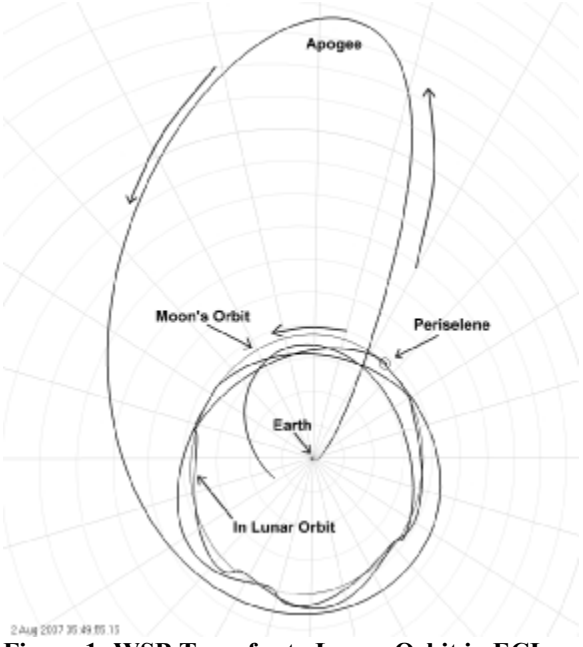

Figure 1: WSB Transfer to Lunar Orbit in ECI

Until 1996 it was difficult to calculate WSB transfers in an efficient way. This is because the dynamics in this region being sensitive make it difficult to target to from the Earth using standard search methods that one might

* Research Mathematician, AIAA Senior Member
Princeton University and Innovative Orbital Design, Inc.
Princeton, New Jersey

† Senior Astrodynamics Specialist
Analytical Graphics, Inc.
Malvern, Pennsylvania

use for Hohmann transfer design. Thus, backwards methods were employed where one would start the targeting process at the lunar WSB, and then integrate backwards and see where the tiny variations in the lunar capture state could cause the trajectory to come back to the Earth at the desired state[1,2,16]. This approach is unwieldy and time consuming. It was discovered in 1993[3] that the backward method works because the trajectories were following invariant manifolds associated to the WSB. It was conjectured in a special case that the WSB was a complicated region consisting of many intersections of invariant manifolds, and this was verified in 1999[12].

In 1996 a standard type forward search algorithm was discovered to compute these transfers[4]. It was developed in support of the US Air Force Academy Blue Moon mission study. It uses only two control variables at the Earth and two target parameters at the Moon. This is referred to as a *forward method* and is used in this paper together with the software package *Astrogator* to show how to calculate these transfers in a straight forward and efficient manner. We demonstrate how to determine a launch period, and other important mission design quantities. The forward algorithm is introduced in Section 2.1. It is applied in a modified form in Sections 3, 4, and 5.

The WSB lunar transfer when compared to a Hohmann transfer has many advantages[4]. If one considers leaving the Earth in a Low Earth Orbit (LEO) at 200 kilometers altitude and transferring to Low Lunar Orbit (LLO) at 100 kilometers altitude, the WSB transfer saves about 25% in the ΔV required for lunar capture, while the ΔV required to leave LEO is about the same. This 25% improvement can in certain circumstances double the payload that can be placed into LLO. Also, the capture process is more gradual not requiring large Newton thrusters, and the sensitivity of the transfer means that less ΔV is required for orbit maintenance. The WSB transfer has the increased flight time of 90 days and an Earth apoapsis of approximately 1.5 million kilometers which should be considered in mission design. This transfer is being considered in a number of mission studies, and plans to be used for Japan's Lunar A mission[10]. Because of the possible doubling payload aspect of these transfers, they may be very advantageous for any future lunar base development. It is noted that these transfers can also be constructed for ballistic capture at Europa's WSB[14], and could be designed for other planets and satellites as well.

The following section describes an overview of the forward targeting algorithm and the definition of the WSB. Section 3 then describes a practical application of this algorithm to calculate a specific WSB transfer from Earth to a lunar orbit. This trajectory was taken as the nominal (or "baseline") trajectory for the subsequent launch window analyses described in sections 4 and 5. Section 6 gives details of *STK/Astrogator's* software models used in these analyses.

2. EFFICIENT FORWARD TARGETING

In this section, the forward targeting algorithm is briefly described, and the WSB is plotted in 3D for a special choice of parameters.

2.1 Forward Targeting Algorithm

The previously published forward algorithm[4] is briefly described here. The trajectories calculated in this algorithm should be numerically integrated modeling the forces acting upon the spacecraft as accurately as possible. An application of this targeting algorithm will be demonstrated in Sections 3, 4, and 5, along with a description of the numerical methods used.

We consider a point **x** with respect to the Earth at a radial distance r_E. The six orbital elements that are chosen at **x** are represented in special spherical coordinates by r_E, longitude (α_E), latitude (δ_E), velocity magnitude (V_E), flight path angle (γ_E), flight path azimuth (σ_E–the angle in the local plane from the projection of the positive z-axis to the velocity vector.) We let r_M, i_M be the desired radial distance and inclination with respect to the Moon. The *2X2* targeting algorithm is to vary V_E, γ_E and target to r_M, i_M. Symbolically, this is denoted by

$$V_E,\ \gamma_E \rightarrow r_M,\ i_M\ .$$

The initial value of V_E is chosen so that the trajectory is on a Keplerian ellipse with an Earth apoapsis of 1.5 million kilometers. The initial value of γ_E is chosen near zero. The initial epoch is chosen so that the Sun is at a desired angular distance away. The method of determining the desired angular distance of the Sun has been previously described[16], and an example will be demonstrated in Section 3. Using a second order Newton's differential correction targeting algorithm it is found that convergence to r_M, i_M usually occurs in about six iterations, and that the resulting lunar eccentricity e_M is less than one, so the state is elliptic and the spacecraft is in the lunar WSB. It is remarked that at the Earth apoapsis of the transfer at approximately 1.5 million kilometers, which occurs about 45 days after Earth injection, the spacecraft is in the WSB of the Earth, where the Sun is the main perturbation. This is different from the WSB of the Moon where the Earth is

the main perturbation. A precise meaning of being in the Earth-Sun WSB has been previously described[6].

2.2 Visualization of Weak Stability Boundaries

The analytic formulation and visualization of WSB's has been given in detail[5,6] and we only summarize a few results relevant for this paper regarding the lunar WSB.

For simplicity for this section alone, we only model the Earth and Moon, and assume that they move about their common center of mass in uniform circular motion. In addition, we assume that the motion of the spacecraft lies in the same plane as the Earth and Moon, and the spacecraft is assumed to have zero mass. We go to a rotating coordinate system whose x-axis passes through the Earth and Moon, and which rotates with the same uniform velocity as the Earth and Moon. We put the center of the coordinate system at the Moon, where the Earth is now located on the x-axis to the right of the Moon. The unit of distance is dimensionless, and scaled so that the average Earth-Moon distance of about 380,000 kilometers is normalized to 1.0. In our two plots below, the actual distance for r_M is obtained by multiplying the scaled distance by 380,000 kilometers. Likewise, the uniform velocity of the Moon about the Earth is normalized to 1 and the mass ratio—the Moon's mass divided by the Earth's mass—is taken to be $\mu = 0.0123$. This is the modeling for the planar restricted three-body problem.

In polar coordinates with respect to the Moon in the rotating system, r_M, θ, the Earth is at the angle $\theta = 0$, and the anti-Earth direction, towards the exterior Lagrange point, is $\theta = \pi$. A quantity that is of interest is the total energy the spacecraft has moving in the scaled rotating system, and it is called the Jacobi energy[5,15]. Here, we use the variable E, which is negative of the Jacobi energy. The variable E has special value of approximately $E_1 = -3.184$ when evaluated at the exterior Lagrange point. We are interested when capture can occur at the Moon and this can only happen when $E > E_1$.

The WSB can be parameterized by e_M, θ, E. More exactly, it gives a distance r_M where a spacecraft orbiting about the Moon is between capture and escape, and where the spacecraft is captured so that $e_M < 1$. Thus, it is an unstable capture. The distance then from the Moon where the WSB is located is

$$r_M = r_M(e_M, \theta, E). \qquad (1)$$

Equation 1 has previously been given implicitly[5,6]. From (1), we can alternatively write

$$E = E(e_M, \theta, r_M). \qquad (2)$$

It is assumed this distance is the periapsis radius, so that the velocity v_M is known from e_M, r_M as

$$v_M = ((1+e_M)\mu)^{1/2} r_M^{-1/2} - r_M . \qquad (3)$$

This is the inertial velocity at periapsis in rotating coordinates.

The WSB is plotted in Figure 2. We plotted the surface $E = E(e_M, r_M)$, where we chose $\theta = \pi$. We chose $\theta = \pi$ because for the WSB transfer, capture at the Moon typically occurs near the lunar far side. In this plot, the vertical z-axis is the E-axis, and this axis starts at $E = E_1$, which is needed since we require $E > E_1$. It is seen that as e_M approaches 1, r_E approaches 0. The x-axis is the e_M-axis, and the y-axis is the r_M-axis. This was plotted with Mathematica. The portion of the plot that is flat means that the surface is below E_1.

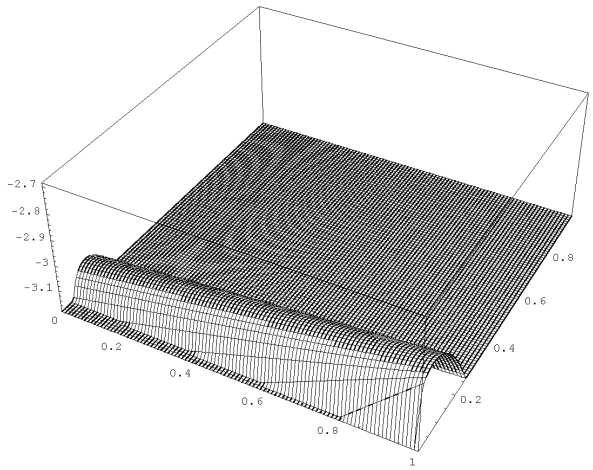

Figure 2: Lunar WSB Surface – (e_M, r_M, E), $\theta = \pi$

If a contour plot is made from this plot for r_M near zero for the values corresponding for capture altitudes of a few hundred kilometers, e.g., $r_M = 0.0059$ corresponds to about 500 kilometer altitude, then Figure 3 is obtained.

The vertical axis is e_M, and the horizontal axis is r_M. Thus, there are many values of E giving rise to points on the WSB where ballistic capture can occur with the given values. In this plot, $E \in [-3.13, -2.98]$. These values agree to high precision when compared to actual ballistic capture transfer values at the WSB. Thus, the analytic formulation previously given[5,6] is an accurate modeling.

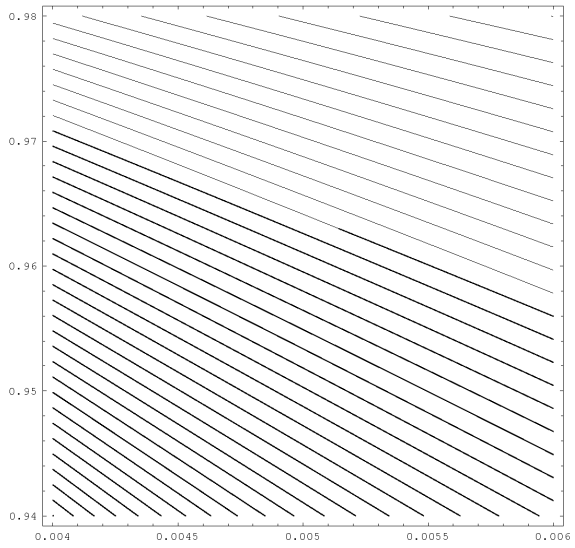

Figure 3: Moon – *E*-contours, (r_M, e_M)-plane

3. THE NOMINAL TRAJECTORY

We generated the nominal trajectory described in the following analysis using a modified form of the forward targeting algorithm previously described. We made these modifications to allow straightforward launch window analysis. The nominal trajectory was calculated for a launch in April, 2007, although these transfers are possible every month. The desired lunar parameters were chosen to be r_M = 3000 kilometers, and i_M = 90 degrees.

We modeled the nominal trajectory using STK/*Astrogator's* "Mission Control Sequence" (*MCS*). The *MCS* allows specification of the "segments" that collectively define the entire trajectory; the user defines any combination of propagation and maneuver segments (along with other segments) and sets the parameters for each segment. For this analysis, we used a sequence that started from launch, inserted into a 300 kilometer circular LEO, and coasted in LEO until the Trans-Lunar Injection (TLI) maneuver. We modeled the TLI as an impulsive ΔV along the velocity vector, and propagated the orbit using numerical integration through the transfer, the capture at the Moon and then in lunar orbit.

3.1 Determining the Launch Date

Once the desired month of launch had been chosen, the first step was to determine the day of the month for launch that would have the required Sun-Earth-Moon geometry. The Sun-Earth-Moon angle, λ, is convenient to describe the geometry. Figure 4 shows λ in the Sun-Earth Rotating coordinate system. The Earth is in the center, and the Sun-Earth line defines the x-axis. The trajectory is the same as in Figure 1. In this analysis we chose a Quadrant II transfer, which has its apogee toward the Sun. (Quadrant IV transfers are also possible, which effectively rotates the geometry by 180 degrees.)

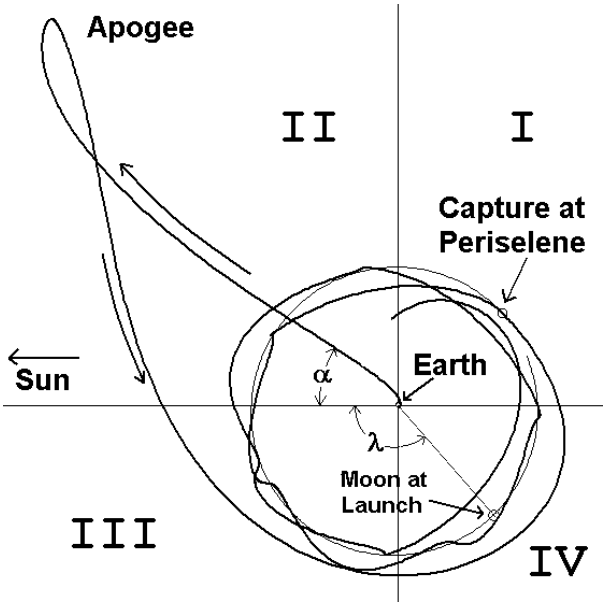

Figure 4: Quadrant II WSB transfer in Sun-Earth Rotating Coordinates.

Using a first guess of λ = 130° for a quadrant II transfer based on previous work[4] is sufficient to allow subsequent targeting steps to converge. Although this can be done manually looking at an almanac, it was convenient to use *Astrogator's* differential corrector targeter to find the date in April, 2007, where λ = 130°. The first date found was 27 April. (7 April yields the same λ.)

3.2 Calculating the Trans-Lunar Injection (TLI) ΔV

The next step is to determine the necessary TLI ΔV to impart the proper energy to leave LEO and enter the transfer trajectory. As mentioned before, the apogee of these transfers is about 1.5 million kilometers. As a first guess using an Earth-centered Keplerian 2-body motion, the semimajor axis, a, of an ellipse with such an apogee radius and a radius of perigee of 6678 kilometers (300 kilometer altitude) is about 753,340 kilometers. From the vis viva equation,

$$\frac{v^2}{2} - \frac{\mu}{r} = -\frac{\mu}{2a}, \qquad (4)$$

(with μ representing, in this case, the gravitational constant of the Earth) the velocity at perigee of this ellipse, v_f is about 10.902 kilometers/second. Since it is easily calculated using (4) that the velocity, v_i, in the 300 kilometer circular LEO is about 7.726 kilometers/second, a first guess at the impulsive TLI ΔV is

$$\Delta V_{TLI} = v_f - v_i = 3.176 \text{ km/second.}$$

Of course, the actual LEO orbit will not be perfectly circular, and sometimes during pre-mission analysis the LEO altitude is not defined very well, so it is often convenient to work in terms of the orbital energy rather than absolute velocities. The definition of the *C3* energy is

$$C3 = -\mu/a,$$

which yields –0.529 km^2 / second^2. A differential corrector can quickly calculate the necessary ΔV_{TLI} from any point in the orbit at any LEO altitude.

3.3 Calculating the Launch and Coast Times

Figure 4 shows the angle, α, between the Sun-Earth line and the trajectory at launch. A first guess at this angle is important for creating a trajectory that will encounter the Moon with the proper arrival conditions. If the trajectory were hyperbolic with respect to the Earth, this angle would be calculated as the angle between the outgoing asymptote and the Sun-Earth line. Because the trajectory is less than hyperbolic, we use the line-of-apsides as the defining parameter. It is convenient to represent the Right Ascension, α, and the Declination, δ, of the line-of-apsides in the Sun-Earth rotating coordinate system. Using this representation, δ becomes a measure of the trajectory's relationship to the ecliptic plane. Moreover, because the Moon's orbit is within 5 degrees of the ecliptic plane, this is a useful parameter to monitor and control.

The time of launch and the coast duration in LEO before TTI fully control the orientation of the post-TLI transfer ellipse. The time of launch establishes the Right Ascension of the Ascending Node (*RAAN*), and the coast duration establishes the argument of perigee, ω. *Astrogator's* targeter quickly modifies these control parameters to converge on a specified α and δ. For Quadrant II transfers, a first guess of α between 25 and 40 degrees is sufficient. We chose $\delta = 0$ degrees as a first guess for simplicity. However, these trajectories are not confined to stay in the ecliptic plane, and other mission requirements may drive the selection of δ.

In section 2.1, the forward targeting algorithm used the control parameters V_E and γ_E to target on the constraint parameters at the Moon. The ΔV_{TLI} directly corresponds to V_E by simply being the difference between V and the velocity in LEO.

The control parameter γ is directly related to the coast duration. Figure 5 shows γ as the angle between the velocity vector, V, and the local horizontal (which is perpendicular to the position vector). We can also choose an equivalent state R' and V', with a corresponding γ' set to zero. R' must be rotated in a retrograde fashion from R by the angle γ in order to align V' along the direction of V. This position of R is directly controlled by the coast duration, which is the time when the spacecraft is in LEO from insertion until TLI. The duration from launch to LEO insertion is assumed to be constant and depends on the launch vehicle.

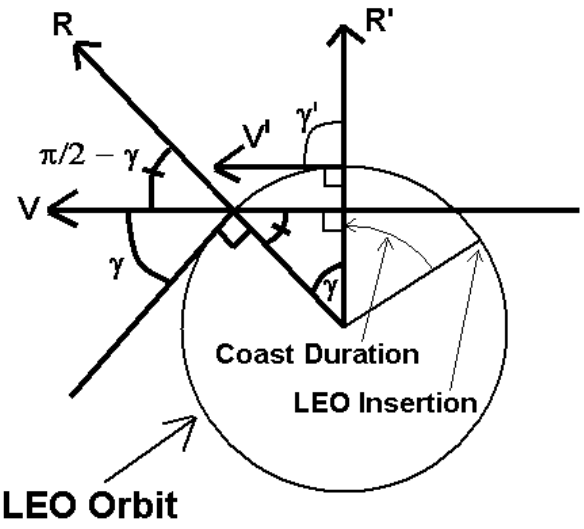

Figure 5: The relationship of flight-path angle to coast duration.

3.4 Targeting the Lunar Capture

Once the launch date, energy, and orientation of the transfer trajectory were determined as previously described, the trajectory arrives at the moon with a radius of lunar periapsis (periselene) from 30,000 kilometers to 250,000 kilometers.

It should be noted that these trajectories experience multiple periselene passages, and care must be taken to monitor the periselene at which the constraint parameters are evaluated. The first periselene encountered by the spacecraft after apogee occurs about a week after apogee, and the spacecraft is about 1.4

million kilometers from the Moon. This periselene is not useful for targeting. The second periselene occurs much closer to the Moon, and can be targeted directly. Unfortunately, because of the sensitive nature of these trajectories, sometimes the second perigee is 200,000 kilometers or more from the Moon, and the third perigee is much closer to the Moon. In this case it was helpful to set up *Astrogator* to stop propagation both on the third periselene, and on the second periselene if the distance from the Moon was less then 50,000 kilometers. *Astrogator* then stops at the first satisfied condition.

At this point, it was sometimes helpful to refine ΔV_{TLI} by first targeting on a constraint of r_M = 10,000 kilometers. This eliminated the problem of stopping on different periselene events during targeting. After this converged, targeting on r_M = 3000 kilometers and i_M = 90 degrees converged more rapidly.

After the targeting on r_M and i_M converged, we had some success in controlling how well the spacecraft was captured in Lunar orbit by increasing the targeting problem from *2x2* to *3x3*, and targeting the *C3* at periselene with respect to the Moon. The additional control parameter was the launch time. After targeting the *2x2* problem, the lunar *C3* measured at periselene was about –0.04 kilometers^2/second^2. We targeted for a *C3* of –0.1, which resulted in the trajectory displayed in Figures 1 and 4. This trajectory orbits the Moon for several months after the initial periselene capture. Investigation of this capability was beyond the scope of this paper, but was promising enough to be used for launch window analysis, described in the next section.

4. LAUNCH WINDOW DURING A SINGLE DAY

For this analysis, the "Launch Window" is defined as the time during a given day that the spacecraft can be launched and return to it's nominal orbit, in this case, around the Moon. Although it is not always necessary to return to the exact same orbit to meet mission requirements, for this analysis it demonstrated useful trends. Returning to the exact same orbit often increases the ΔV unnecessarily if only a few orbit parameters are required.

Using the trajectory targeted in the previous section, we looked at launching before and after the nominal launch time. Since it is unlikely that the LEO coast duration and the ΔV_{TLI} can be changed when the launch slips on the order of a few minutes, these parameters were not used to retarget the trajectory. Instead, a Mid-Course Correction Maneuver, (MCCM), was placed at apogee. Three orthogonal components of MCCM were described using *Astrogator's* Velocity-Normal-Conormal (VNC) local coordinate axes. The x-axis of this system is defined to be aligned with the inertial velocity vector, $\boldsymbol{V}$. The y-axis is aligned with the orbit angular moment, $\boldsymbol{N} = \boldsymbol{R}\text{x}\boldsymbol{V}$. The z-axis is called the "conormal", and is defined as $\boldsymbol{C} = \boldsymbol{V}\text{x}\boldsymbol{N}$. $\boldsymbol{C}$ is therefore directed outward, away from the central body of the orbit. For a circular orbit or at apoapsis and periapsis, $\boldsymbol{C}$ is naturally aligned with $\boldsymbol{R}$.

The nominal launch time was varied by 10 minutes, before and after. Each trajectory was targeted back to the same lunar orbit. This targeting was done in three steps. These steps were automated in *Astrogator* so no user intervention was necessary between them.

First, the conormal component of MCCM was controlled to target a constraint that when the spacecraft was within 300,000 kilometers of the Moon, the distance from the Earth was the nominal value of 555,610 kilometers.

The second step controlled the normal and conormal components of MCCM to target on constraints at periselene: r_M = 3000 kilometers, i_M = 90 degrees.

The final step was to add the velocity component of MCCM to the controls of step 2, and add the constraint of lunar *C3* = -0.12 kilometers^2/second^2.

Figure 6 shows a linear dependence of the MCCM ΔV on the time from launch. These data indicate that a launch window of 20 minutes on this day could be achieved for a possible ΔV of less than 50 meters/second.

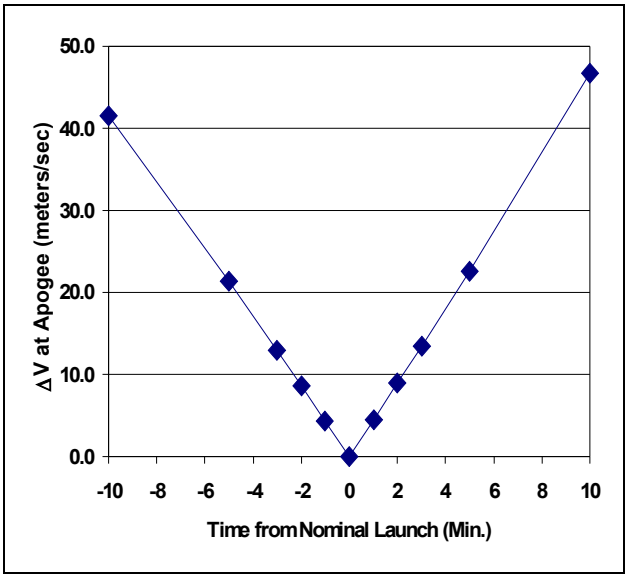

Figure 6: MCCM ΔV as a Funtion of Launch Time

There is no reason to think that apogee is the optimal place to perform this MCCM. We varied the true anomaly of MCCM on one occasion by plus and minus two degrees, and saw a change in MCCM magnitude of a few meters per second. For the sake of consistency, all were performed at apogee in this study, but further investigation could prove useful.

The Launch, ΔV, and Periselene data for these cases are given in Table 1 in the Appendix.

5. LAUNCH PERIOD OVER SEVERAL DAYS

This section describes the "Launch Period", which we define for this analysis as the days of the month that the spacecraft can be launched and return to it's nominal orbit. As with the previous launch window study, we assume that the TLI ΔV magnitude cannot be changed from day to day. However, we assume that the coast duration in LEO can be reprogrammed on the launch vehicle, and therefore we used it as a control parameter.

Because the Moon moves about 13 degrees every day, there is a serious timing problem in trying to return to a nominal orbit. A single maneuver at apogee will not correct the orbit for a one-day launch slip; the period of the transfer orbit must be changed. We used an "Energy Correction Maneuver" (ECM) to accomplish this change in period. The ECM was applied along the inertial velocity direction using the VNC axes, and can be positive (direct) or negative (retrograde).

The most efficient place to change the period of an elliptical orbit is at periapsis, which is where the TLI occurs. In maneuver operations, the maneuver cannot be planned until a good orbit state vector is produced from tracking the spacecraft and performing orbit determination. For orbits with high eccentricity, the orbit determination solution requires from 4 to 12 hours of tracking. For this analysis, we assume that no maneuver can be performed until after 24 hours from TLI. (If the maneuver can be performed earlier, the ΔV will be less than reported here.)

In addition to the ECM, the MCCM from the previous section was also used. This with the time of launch and the coast duration give six control parameters:

1. Launch epoch,
2. Coast duration in LEO,
3. ECM velocity component,
4. MCCM velocity component,
5. MCCM normal component, and the
6. MCCM conormal component.

With such a variety of control parameters, we can expect a unique solution to the targeting problem with a like number of constraints. After inspection of the perturbed trajectories and some experimentation it was found that the easiest place to target constraints was not at periselene, but at 300,000 kilometers from the Moon. At this point we targeted on the remaining 6 parameters that made up the nominal state vector at this same radius, represented with respect to a Moon-centered inertial coordinate system as:

1. Epoch,
2. Right Ascension,
3. Declination,
4. Lunar *C3*,
5. horizontal flight path angle, and
6. inertial velocity flight path azimuth.

This *6x6* targeting method converged very rapidly for the "nominal plus 1 day" case, and up to the "nominal minus 3 day" cases. Figure 7 shows the relationship of the total ΔV (ECM + MCCM) to the days from the nominal launch.

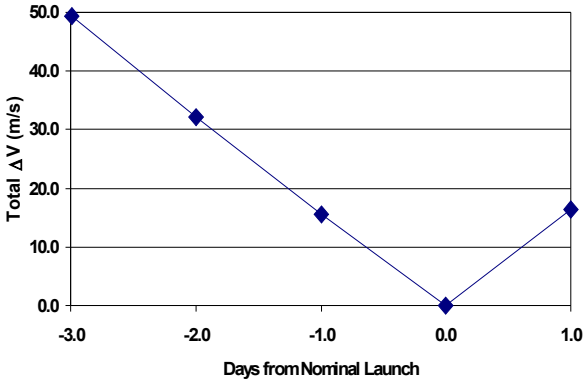

Figure 7: Total ΔV as a Function of Launch Date

These data indicate that a 5-day launch period including the nominal could be achieved for a possible ΔV of 50 meters/second

The "nominal plus 2 day" case and the "nominal minus 4 day case" converged very slowly, but are not even reported here because they never converged completely, and the MCCM ΔV was growing in excess of 500 meters/second. Perhaps other maneuver strategies would allow these to converge for a reasonable ΔV cost.

The Launch, ΔV, and Periselene parameters for these cases are given in Table 2 in the Appendix.

6. SOFTWARE MODELS

The software used in this analysis is the *Satellite Tool Kit* (*STK*). *STK/Astrogator* is the maneuver planning and trajectory design module of STK. Additionally, the *Visualization Module* (*VO*) was used extensively to analyze the complex 3-dimensional nature of the trajectories as they fall towards the Moon. (More detailed descriptions of *Astrogator's* algorithms can be found in the on-line help.)

STK/Astrogator was developed commercially by Analytical Graphics, Inc., in cooperation with the Flight Dynamics Analysis Branch at the NASA Goddard Space Flight Center (GSFC). *Astrogator* was developed as a commercial follow-on to the software program *Swingby*[7,8,17], previously developed at GSFC.

6.1 Launch Model

STK/Astrogator uses a simple launch model to support this type of analysis. The launch model is configured with the LEO insertion, or "burnout" state vector, represented relative to the Earth-body-fixed system. These parameters are normally obtained by the trajectory analyst from the launch vehicle organization. In addition to the burnout parameters, the time-of-flight from launch to burnout is entered. By making the assumption that the burnout state will remain the same with respect to the Earth-body-fixed system for a wide range of launch times and days, *Astrogator* adds the time-of-flight to the launch epoch, rotates the body-fixed state to an inertial coordinate system, and uses this as the initial state vector for the LEO. This allows all targeting to be done in a forward manner, and the analyst does not need to try to "patch" a trajectory back to a launch inclination and RAAN.

6.2 Orbit Propagation

There are several user-configurable orbit propagation algorithms in *STK/Astrogator*. They all consist of variable step Runge-Kutta numerical integrators, and for this study, the Cowell form of the equations of motion were integrated. The analyst configures the force model through the user interface, and can select from a variety of options: The central body of integration; the spherical harmonic model used along with the degree and order; the atmospheric model; 3rd body perturbations; and solar radiation pressure.

For this study, the positions of the planets were calculated from the Jet Propulsion Laboratory's DE-405 ephemerides (although other theories can be substituted).

6.3 Targeting

The targeting algorithm used in *Astrogator* is a differential corrector. This calculates a numerical sensitivity matrix describing the changes in the constraints as a function of changes in the controls. This matrix is used to estimate the corrections to the control variables based on the deviations from the desired constraints. The user has control over the perturbation size used to calculate the numerical partial derivatives, as well as several other options to control the speed of convergence. This technique has proven useful on a variety of missions, and the implementation in *Astrogator* has features so that the process can be automated though the GUI and through scripts.

CONCLUSIONS

We have shown examples of how WSB transfer trajectories can be targeted with readily available software. We have also demonstrated that it is possible to return achieve a nominal lunar orbit for a 20 minute launch window on a given day for about 50 meters/second ΔV. Furthermore, for and additional 50 meters/second a launch period of about 5 days per lunar cycle can be achieved.

We are optimistic that by using other trajectory techniques, the launch opportunities can be expanded, and the ΔV cost reduced. Other options include using cislunar loops to correct launch errors and launch slips before transferring to the large orbit. The placement of the corrective maneuvers ECM and MCCM can be adjusted to reduce ΔV. And possibly most significantly, if the mission can be accomplished with loose requirements on the lunar orbit, a "return-to-nominal" method can be avoided, which could substantially reduce the ΔV costs.

ACKNOWLEDGEMENTS

The first author was supported in part by a contract with the Jet Propulsion Laboratory, California Institute of Technology, and NASA.

REFERENCES

1. E.A. Belbruno, "Lunar Capture Orbits, A Method of Constructing Earth-Moon Trajectories and the Lunar GAS Mission," in: *Proceedings of AIAA/DGLR/JSASS Inter. Propl. Conf.*, AIAA Paper No. 87-1054, (May 1987).

2. E.A. Belbruno, J. Miller, "Sun-Perturbed Earth-to-Moon Transfers with Ballistic Capture," J. Guid., Control and Dynamics, **16**, No. 4 (July--August 1993) 770-775.

3. E.A. Belbruno, "The Dynamical Mechanism of Ballistic Lunar Capture Transfers in the Four-Body Problem from the Perspective of Invariant Manifolds and Hill's Regions," *Institut D'Estudis Catalans*, CRM Research Report No. 270, (November 1994).

4. E.A. Belbruno, R. Humble, J. Coil, "Ballistic Capture Lunar Transfer Determination for the U.S. Air Force Academy Blue Moon Mission," *Advances in Astronautical Science, Spaceflight Mechanics*, **95**, AAS Publ., Paper No. AAS 97-171, (1997).

5. E.A. Belbruno, "Low Energy Trajectories for Space Travel and Stability Transition Regions," in *Proceedings of IFAC Workshop on Lagrangian and Hamiltonian Methods for Nonlinear Control*, IFAC Publ., Elsevier Science Ltd., Oxford (March 2000) 7-12.

6. E.A. Belbruno, "Analytic Estimation and Geometry of Weak Stability Boundaries with Several Mission Applications", *JPL Contract no. 1213585: JPL Interim Report no. 2*, (June 16, 2000).

7. J. Carrico et al., "Rapid Design of Gravity Assist Trajectories," *Proceedings of the ESA Symposium on Spacecraft Flight Dynamics*, Darmstadt, Germany, (October 1991). 427-434

8. J. Carrico et al., "An Interactive Tool for Design and Support of Lunar, Gravity Assist, and Libration Point Trajectories," AIAA/AHS/ASEE Aerospace Design Conference, Irvine, California, AIAA Paper No. 93-1126, (February 1993).

9. G. Gomez, J. Llibre, R. Martinez, C. Simo, "Station Keeping of Libration Point Orbits," *Final Report: ESOC Contract 5648/83/D/JS(SC)*, (1985).

10. J. Kawaguchi, H. Yamakawa, T. Uesugi, H. Matsuo, "On Making Use of Lunar and Solar Gravity Assists in Lunar-A, Planet B Missions," *Acta. Astr.*, **35**, (1995) 633-642.

11. J. Kawaguchi, "On the Weak Stability Boundary Utilization and its Characteristics," in: *Proceedings of 2000 AAS/AIAA – Spaceflight Mechanics Meeting*, AAS/AIAA Paper No. 00-176, (January 2000).

12. W.S. Koon, M.W. Lo, J.E. Marsden, S.D. Ross, "Heteroclinic Connections between Periodic Orbits and Resonance Transitions in Celestial Mechanics," (Preprint, 1999).

13 P.A. Penzo, "A Survey and Recent Developments of Lunar Gravity Assist," in: *Space Manufacturing 12, Proceedings of the SSI Princeton Conference on Space Manufacturing*, (2000).

14 T. Sweetser, et. al., "Trajectory Design for a Europa Orbiter Mission: A Plethora of Astrodynamic Challenges," in: *Proceedings of AAS/AIAA Space Flight Mechanics Meeting*, Paper No. AAS 97-174, (February 1997).

15 V. Szebehely, *Theory of Orbits*, (Academic Press, 1967).

16 H. Yamakawa, J. Kawaguchi, N. Ishii, H. Matsuo, "On Earth-Moon Transfer Trajectory with Gravitational Capture," in: *Proceedings AAS/AIAA Astrodynamics Specialists Conf.*, Paper No. AAS 93-633, (August 1993).

17 J. Carrico , D. Conway , D. Ginn, K. Richon, D. Folta, "Operational Use of Swingby—An Interactive Trajectory Design and Maneuver Planning Tool—for Missions to the Moon and Beyond," *AAS/AIAA Astrodynamics Specialist Conference*, Halifax, Nova Scotia, AAS Paper No, AAS 95-323 (August, 1994)

APPENDIX: TABLES

The data in these tables have the following units:

- *ΔT* in minutes and seconds, as noted;
- *ΔV* in meters/second;
- distance in kilometers;
- *C3* in kilometers^2/second^2; and
- angles in degrees.

Launch Epoch	ΔT (min)	MCCM ΔV (m/s)	Periselene Parameters								TOF (Days)
			Rp	Inc	C3	Ecc	RAAN	ω	Epoch	ΔT (s)	
4/27/07 21:42	-10.00	41.52	2999.999	90.0000	-0.1206	0.9262	84.6346	10.7149	8/2/07 4:45	-64.90	-96.29
4/27/07 21:47	-5.00	21.36	3000.022	90.0001	-0.1206	0.9262	85.1526	13.2575	8/2/07 5:30	-19.59	-96.32
4/27/07 21:49	-3.00	12.97	3000.892	89.9958	-0.1206	0.9262	85.3038	14.2513	8/2/07 5:41	-8.53	-96.33
4/27/07 21:50	-2.00	8.69	3000.024	90.0001	-0.1206	0.9262	85.3703	14.7454	8/2/07 5:45	-4.78	-96.33
4/27/07 21:51	-1.00	4.37	3000.014	89.9996	-0.1206	0.9262	85.4267	15.2353	8/2/07 5:48	-1.91	-96.33
4/27/07 21:52	0.00	0.00	3000.965	90.0044	-0.1206	0.9262	85.4785	15.7209	8/2/07 5:49	0.00	-96.33
4/27/07 21:53	1.00	4.43	2999.974	89.9998	-0.1206	0.9262	85.5164	16.2065	8/2/07 5:50	0.77	-96.33
4/27/07 21:54	2.00	8.90	3000.009	90.0001	-0.1206	0.9262	85.5492	16.6877	8/2/07 5:50	0.60	-96.33
4/27/07 21:55	3.00	13.44	3000.001	90.0000	-0.1206	0.9262	85.5738	17.1663	8/2/07 5:49	-0.60	-96.33
4/27/07 21:57	5.00	22.67	3000.016	90.0000	-0.1206	0.9262	85.5989	18.1155	8/2/07 5:43	-6.03	-96.32
4/27/07 22:02	10.00	46.76	3000.151	89.9995	-0.1206	0.9262	85.5200	20.4460	8/2/07 5:12	-37.07	-96.30

Table 1: Launch Window During a Single Day–Launch, ΔV, Periselene Data, and Time-of-Flight (TOF)

Launch	Coast	ECM ΔV	MCCM ΔV	Total ΔV	Periselene Parameters								TOF
ΔT (days)	(min)	(m/s)	(m/s)	(m/s)	Rp	Inc	C3	Ecc	RAAN	ω	Epoch	ΔT (s)	(days)
-2.99	17.01	3.3379	46.0729	49.4108	2998.523	88.5977	-0.1199	0.9266	84.7838	15.7710	8/2/07 6:35	45.53	99.36
-1.99	17.17	2.3589	29.7187	32.0776	2998.575	88.6061	-0.1200	0.9266	84.7878	15.7706	8/2/07 6:35	45.22	98.36
-1.00	17.34	1.2081	14.3295	15.5376	2998.634	88.6044	-0.1200	0.9266	84.7869	15.7708	8/2/07 6:35	45.22	97.36
0.00	17.53	0.0000	0.0000	0	3000.968	90.0044	-0.1206	0.9262	85.4785	15.7209	8/2/07 5:49	0.00	96.33
1.00	17.74	1.6353	14.6953	16.3306	2998.490	88.7504	-0.1200	0.9266	84.8589	15.7646	8/2/07 6:30	40.52	95.36

Table 2: Launch Period Over Several Days–Launch, ΔV, Periselene Data, and TOF.